nature medicine

Viral variants that initiate and drive maturation of V1V2-directed HIV-1 broadly neutralizing antibodies

Jinal N Bhiman[1,2], Colin Anthony[3], Nicole A Doria-Rose[4], Owen Karimanzira[1], Chaim A Schramm[5], Thandeka Khoza[1], Dale Kitchin[1], Gordon Botha[3], Jason Gorman[4], Nigel J Garrett[6], Salim S Abdool Karim[6], Lawrence Shapiro[4,5], Carolyn Williamson[3,6,7], Peter D Kwong[4], John R Mascola[4], Lynn Morris[1,2,6] & Penny L Moore[1,2,6]

The elicitation of broadly neutralizing antibodies (bNAbs) is likely to be essential for a preventative HIV-1 vaccine, but this has not yet been achieved by immunization. In contrast, some HIV-1-infected individuals naturally mount bNAb responses during chronic infection, suggesting that years of maturation may be required for neutralization breadth[1–6]. Recent studies have shown that viral diversification precedes the emergence of bNAbs, but the significance of this observation is unknown[7,8]. Here we delineate the key viral events that drove neutralization breadth within the CAP256-VRC26 family of 33 monoclonal antibodies (mAbs) isolated from a superinfected individual. First, we identified minority viral variants, termed bNAb-initiating envelopes, that were distinct from both of the transmitted/founder (T/F) viruses and that efficiently engaged the bNAb precursor. Second, deep sequencing revealed a pool of diverse epitope variants (immunotypes) that were preferentially neutralized by broader members of the antibody lineage. In contrast, a 'dead-end' antibody sublineage unable to neutralize these immunotypes showed limited evolution and failed to develop breadth. Thus, early viral escape at key antibody-virus contact sites selects for antibody sublineages that can tolerate these changes, thereby providing a mechanism for the generation of neutralization breadth within a developing antibody lineage.

The identification of bNAbs against genetically diverse viruses such as HIV-1 (ref. 9), together with in-depth longitudinal evolutionary studies are providing key insights for vaccine design[7,8,10–12]. BNAbs to the variable regions 1 and 2 (V1V2) of the HIV-1 envelope (Env) are among the most prevalent and potent cross-reactive antibodies, but the virological events that allow for their elicitation and maturation remain unclear. We have previously described the CAP256-VRC26 mAb lineage, isolated from an HIV-1 subtype C–superinfected individual, which targets the V1V2 C-strand at the apex of the viral envelope glycoprotein (**Fig. 1a**)[7]. This lineage developed from a bNAb precursor or unmutated common ancestor (UCA) with a 35–amino acid heavy chain complementarity determining region 3 (CDRH3), and it acquired breadth through moderate levels of somatic hypermutation (SHM)[7]. To better define the complex viral populations responsible for eliciting these antibodies and driving their maturation, we performed next-generation sequencing (NGS) at 28 different time points over 4 years (with an average of 85,000 reads and 788 consensus sequences per time point). From 6–13 weeks, all sequences were closely related to the primary infecting virus (PI) (**Fig. 1b** and **Supplementary Fig. 1**), but at 15 weeks, when superinfection (SU) occurred, there was a dramatic shift in viral populations, with SU-like viruses accounting for 99.8% of 3,228 consensus sequences (**Supplementary Fig. 2**). From 17 weeks, V1V2 sequences from the PI and SU viruses persisted, rapidly forming a PI-SU recombinant population, although PI-like viruses dominated briefly at 23 weeks, perhaps as a result of immune escape from earlier non-V1V2-directed neutralizing antibodies that preferentially neutralized SU-like viruses[13]. Notably, diversification in all three viral populations (PI, SU and recombinants) increased after the CAP256-VRC26 lineage was first detected in blood by NGS at 34 weeks (**Fig. 1b** and **Supplementary Fig. 3**).

As residues 169 and 166 in the V1V2 C-strand form a crucial part of the CAP256-VRC26 bNAb epitope and are likely to be important in virus-mAb co-evolution, we focused on defining escape mutations at these positions. Residue 169 differed between the PI (169Q) and SU viruses (169K), with the majority of viral variants circulating after 23 weeks possessing a PI-derived 169Q mutation (**Fig. 1c** and **Supplementary Fig. 2**). From 27 weeks onwards, the virus sampled 11 different amino acids at position 169, and variation was most pronounced at 42 weeks (**Fig. 1c**), shortly before the development of neutralization breadth. The major escape pathway from 42–119 weeks was a 169I mutation, and thereafter 169E dominated. Toggling was also observed at position 166 (**Fig. 1d**), although this occurred later, with the wild-type 166R immunotype

[1]Centre for HIV and STIs, National Institute for Communicable Diseases (NICD) of the National Health Laboratory Service (NHLS), Johannesburg, South Africa. [2]Faculty of Health Sciences, University of the Witwatersrand, Johannesburg, South Africa. [3]Institute of Infectious Disease and Molecular Medicine, University of Cape Town, Cape Town, South Africa. [4]Vaccine Research Center, National Institute of Allergy and Infectious Diseases, National Institutes of Health, Bethesda, Maryland, USA. [5]Department of Biochemistry and Systems Biology, Columbia University, New York, New York, USA. [6]Centre for the AIDS Programme of Research in South Africa (CAPRISA), University of KwaZulu Natal, Durban, South Africa. [7]National Health Laboratory Services, Johannesburg, South Africa. Correspondence should be addressed to P.L.M. (pennym@nicd.ac.za).

Received 20 May; accepted 3 September; published online 12 October 2015; doi:10.1038/nm.3963

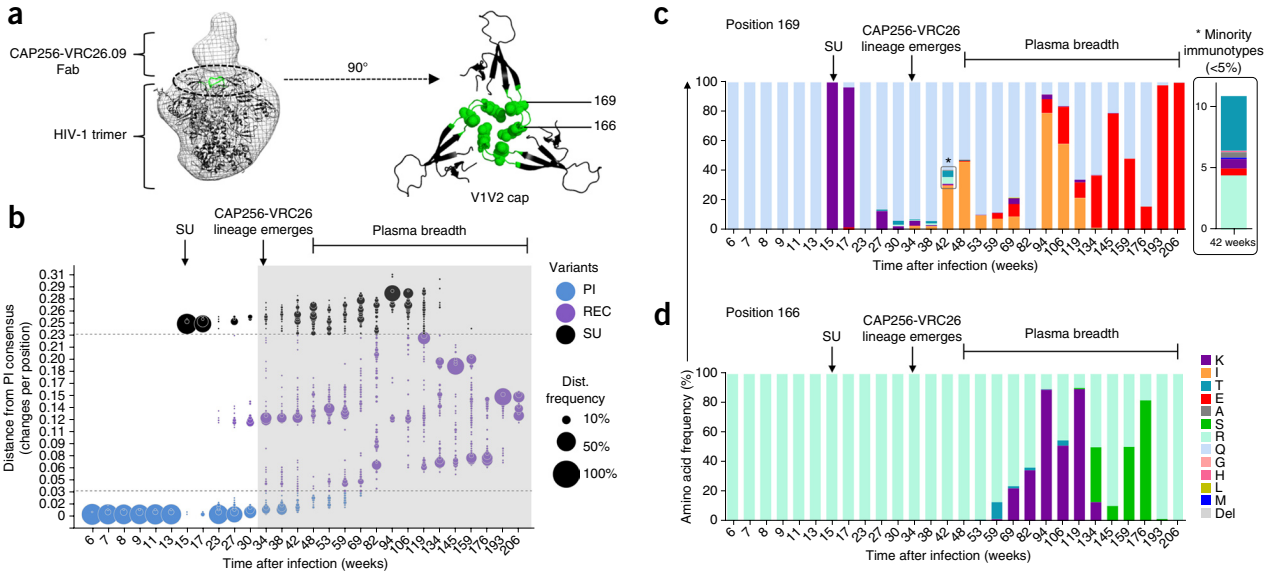

Figure 1 Viral diversification over time in CAP256 HIV-1 Env V1V2. (**a**) BG505 SOSIP.664 trimer structure (PDB: 4TVP) fitted into a 3D reconstruction of the CAP256-VRC26.09 fragment antigen-binding (Fab)-trimer complex (EMD-5856, left). BG505 V1V2 cap with residues 166 and 169 shown as spheres and the C-strand highlighted in green (right). (**b**) Hamming distance from the PI sequence (*y* axis) versus weeks after infection (*x* axis) for all next-generation V1V2 consensus sequences. Values <0.03 and >0.23 were used to distinguish PI-like (blue) and SU-like (black) viruses respectively, whereas those sequences with an intermediate distance (0.03–0.23) were classified as PI-SU recombinant viruses (purple, REC). Hamming distances were normalized for sequence length, and the relative frequency of sequences with a given distance are indicated by the size of the circle (normalized for depth of sequencing, but not for viral load; see **Supplementary Fig. 1**). CAP256-VRC26 next-generation transcript detection in the blood is shown by gray shading. (**c**,**d**) The frequency of amino acids (*y* axis) at positions 169 (**c**) and 166 (**d**) are shown as stacked bars, with each bar representing a single time point from 6 to 206 weeks after infection (*x* axis). Amino acids are colored as indicated, with Del representing a deletion. The inset (*) in **c** expands the 42-week time point (when nine immunotypes are present), to highlight the minority immunotypes present at frequencies of <5%. The time of SU, the emergence of CAP256-VRC26 NGS transcripts and onset of plasma breadth are shown.

(present in both the PI and SU viruses) occurring in more than 98% of sequences until 53 weeks. At 59 weeks, the virus sampled four amino acids (166R, T, K or S), and thereafter 166K, followed by 166S, became prevalent. By 159 weeks, all viral sequences contained the mutually exclusive K169E or R166S mutations. As both the K169E and R166S mutations abrogate neutralization by the CAP256-VRC26 mAbs[7,13] it is unclear why it took two years for these escape pathways to dominate despite their low-level presence early in the development of the CAP256-VRC26 family (**Supplementary Fig. 2**).

The CAP256-VRC26 UCA was unable to neutralize any of 196 HIV-1 isolates (**Supplementary Fig. 4**), suggesting that Env variants able to engage this UCA may be rare. Because CAP256-VRC26 NGS transcripts were first detected in blood 19 weeks after superinfection (**Supplementary Fig. 3**), we analyzed contemporaneous (34-week) viral sequences to identify a bNAb-initiating Env. Neutralization of the SU virus, but not the PI virus, by the CAP256-VRC26 UCA indicated that an SU-like variant elicited this lineage[7]. Although 8% (75/937) of V1V2 next-generation sequences at the 34-week time point were SU-like, none were identical to the SU virus (**Fig. 2a** and **Supplementary Fig. 5**). Single-genome amplification was therefore used to isolate six functional 34-week Env clones, which differed from the SU virus by 2–8 amino acids in V1V2 and by up to 26 changes across the entire Env (**Fig. 2b**). We observed evidence of early immune pressure, with three of six clones containing K169I or K169E mutations, and four of six clones deleting or shifting the glycan at residue 139 (**Fig. 2c**). As expected, the clones with 169I or 169E mutations were resistant to neutralization by the UCA; however, the three clones containing a wild-type 169K were 5–17-fold better neutralized than the SU virus (**Fig. 2d**). Thus, the 34-week viral variants that evolved from the CAP256 SU T/F virus (but differed from the T/F virus by at least 12 amino acids) provided a stronger stimulus for the CAP256-VRC26 lineage.

We next sought to define how this lineage matured to acquire neutralization breadth in the context of CAP256 viral diversification. A heavy chain phylogenetic tree of 33 isolated CAP256-VRC26 mAbs (12 previously described[7] and 21 recently isolated mAbs[14]) and CAP256-VRC26 NGS transcripts from 34 to 206 weeks showed an early bifurcation[7] (**Fig. 3a**). A small sublineage of 34–59-week sequences, including the CAP256-VRC26.01 and 0.24 mAbs, exhibited restricted evolution. A second larger sublineage, containing transcripts from all time points as well as most of the mAbs (**Fig. 3a**), displayed extensive evolution, suggesting adaption in response to emerging viral escape mutations, such as K169T/I/Q/R and R166K (**Fig. 1c**,**d**). To test this hypothesis, we introduced these immunotypes into the SU virus and assayed them against 32 mAbs (CAP256-VRC26.20 does not neutralize SU and was excluded). The CAP256-VRC26.01 and 24 mAbs, from the smaller sublineage with limited breadth, both neutralized the SU virus at 0.04 μg/ml (**Fig. 3b**). However, SU viruses containing the 166 or 169 immunotypes were either neutralization resistant or showed a >670-fold reduction in neutralization sensitivity (**Fig. 3b**). Thus, the inability of mAbs in this dead-end sublineage to tolerate viral escape mutations was likely to be responsible for limiting their evolution and capacity to become broadly neutralizing.

Among the 30 CAP256-VRC26 mAbs from the evolving sublineage that showed a range of neutralization breadth (2–63%), the 169T, 169I or 169Q mutations abolished or reduced the activity of mAbs with limited breadth (**Fig. 3c**). In contrast, the neutralizing activity of broader family members was largely unaffected. This observation was

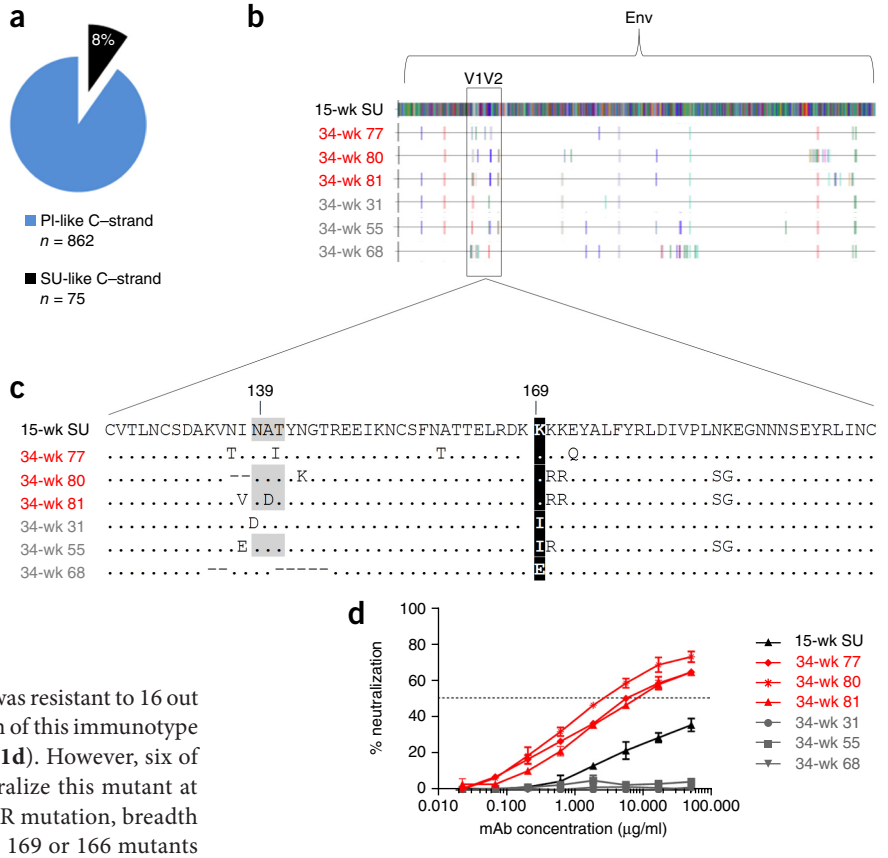

Figure 2 Characterization of the CAP256 34-week Envs. (**a**) Frequency of 34-week next-generation V1V2 consensus sequences possessing a C-strand derived from the PI (blue, $n = 862$) or SU (black, $n = 75$) viruses. (**b**) Amino acid highlighter plot of single-genome amplification (SGA)-derived Env, comparing six SU-like 34-week clones (77, 80, 81, 31, 55 and 68) to the SU virus (designated as the master). Mismatches from the SU are shown as colored ticks and the V1V2 region is boxed. (**c**) Amino acid sequence alignment of the V1V2 region (HXB2 residues 126–196) comparing the SU and the six SGA-derived SU-like 34 week sequences. Red font denotes clones with a wild-type K169, whereas gray font indicates sequences with 169I or 169E mutations. Amino acid identity to the SU virus is represented by dots, deletions are shown as dashes and glycosylation sequons are shaded in gray. (**d**) CAP256-VRC26 UCA neutralization (*y* axis) of the SU virus (black) and the 34-week clones with 169K (red) and 169I or 169E (gray). UCA mAb concentration is shown on the *x* axis. Bars indicate s.e.m. (triplicate).

more pronounced for the R166K mutant, which was resistant to 16 out of 30 mAbs (**Fig. 3c**), consistent with the selection of this immunotype during later stages of bNAb development (**Fig. 1d**). However, six of the nine broadest mAbs were still able to neutralize this mutant at titers <1 μg/ml. With the exception of the K169R mutation, breadth was correlated with the ability to neutralize the 169 or 166 mutants (**Fig. 3c** and **Supplementary Fig. 6**). Overall mAbs with limited neutralization breadth were most severely affected by variation at positions 169 and 166, whereas the broadest mAbs were able to tolerate these early viral escape mutations, thus providing a mechanism for the evolution of neutralization breadth within this lineage.

Because high levels of SHM are often required for HIV-1 broad neutralization[15,16], we investigated the relationship between SHM and neutralization breadth in the CAP256-VRC26 family (**Fig. 4a**). As expected, the nine mAbs with >40% breadth were 17–22% mutated from the UCA; however, three 'off-track' mAbs with a similar level of

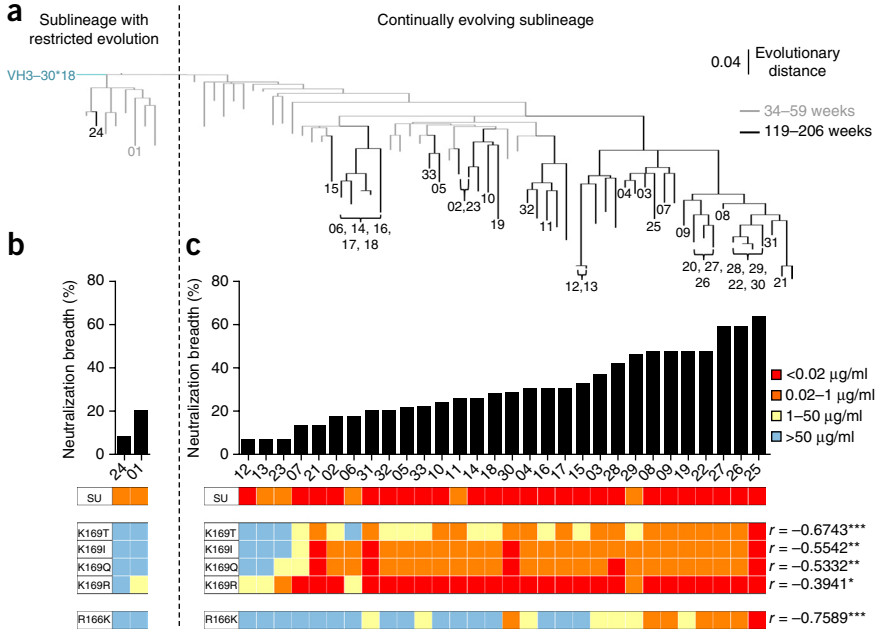

Figure 3 Relationship between bNAb phylogeny, neutralization breadth and tolerance of multiple immunotypes at positions 169 and 166. (**a**) A condensed heavy chain phylogenetic tree, rooted on the VH3-30*18 germline gene and displaying the positions of the 33 CAP256-VRC26 mAbs. Antibody and mAbs are colored according to whether they were isolated from 34–59 weeks (gray) or 119–206 weeks (black). The tree bifurcates into two sublineages (separated by a dashed line); one showing restricted evolution (left) contains only antibody transcripts from early time-points, whereas a continually evolving sublineage (right) contains transcripts from all time points. Scale shows the rate of nucleotide change between nodes. (**b**) Dead-end mAbs in the sublineage with restricted evolution are ranked according to percentage neutralization breadth in the histogram. Neutralization of the SU virus and 169- and 166-mutant viruses by CAP256-VRC26.01 and 24 are shown as a heat map, with shading showing neutralization potency, as indicated in the key. (**c**) Thirty mAbs in the continually evolving sublineage are ranked according to neutralization breadth in the histogram. Neutralization of the SU virus and 169- and 166-mutant viruses by CAP256-VRC26 mAbs are shown as a heat map, with shading showing neutralization potency, as indicated in the key. Correlations (*r*) between neutralization breadth and the IC_{50} titers of each mutant virus are indicated on the right of the heat map. $^{*}P < 0.05$; $^{**}P < 0.005$; $^{***}P < 0.0001$, calculated using a two-tailed non-parametric Spearman correlation.

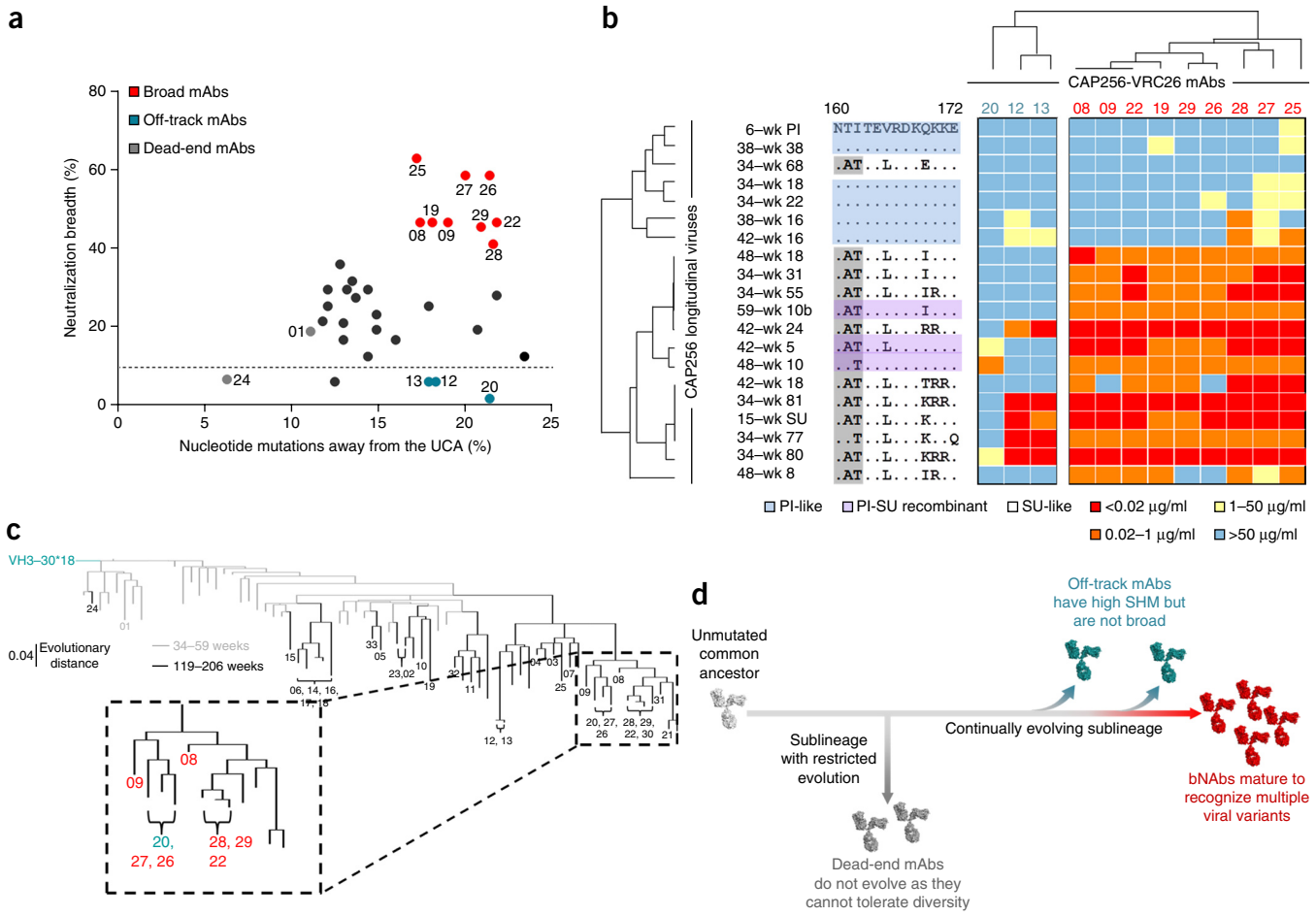

Figure 4 Viral variants that shaped the maturation of broad and off-track antibodies. (**a**) Relationship between neutralization breadth of CAP256-VRC26 mAbs (%, *y* axis) and mutations away from the UCA (%, *x* axis). Broad mAbs with >40% neutralization breadth, off-track mAbs with limited neutralization breadth (<6%) and dead-end mAbs are shown in red, turquoise and gray respectively. The remaining 19 mAbs are shown in black. (**b**) CAP256-VRC26 mAbs and longitudinal CAP256 viruses isolated between 6–59 weeks are hierarchically clustered by their neutralization profiles. Neutralization sensitivity is shown as a heat map with potency indicated in the key. The sequence alignment shows viral C-strand amino acid residues between positions 160–172 (HXB2 numbering), shaded to designate sequences that are PI derived (blue shading), PI-SU recombinants (purple shading) or SU derived (no shading). Off-track (turquoise) and broad (red) mAbs are clustered separately, whereas longitudinal viral variants are clustered by neutralization sensitivity, largely segregated on the basis of an SU-derived V1V2 C-strand. (**c**) A condensed heavy chain phylogenetic tree (**Fig. 3**) with a single clade expanded to illustrate the phylogenetic relatedness of an off-track mAb (turquoise) to seven broad mAbs (red). (**d**) Schematic depicting how CAP256 viral evolution results in the engagement of the CAP256-VRC26 UCA (light gray) and the subsequent development of two distinct mAb sublineages. The sublineage with restricted evolution contains dead-end mAbs (dark gray), which cannot tolerate viral escape mutations. The continually evolving sublineage contains bNAbs (red) and off-track mAbs (turquoise). Although both bNAbs and off-track mAbs have high levels of SHM, only the former mature to recognize multiple immunotypes, and thus acquire breadth.

SHM (17–21%) had only 2–6% breadth (**Fig. 4a**). Therefore, as observed in several families of HIV-specific antibodies[17–20] and influenza-specific antibodies[21], high levels of SHM in the CAP256-VRC26 lineage were not sufficient to confer breadth. To determine whether different viral variants drove the evolution of broad versus off-track mAbs, we tested both groups of mAbs against longitudinal CAP256 viruses (**Fig. 4b**). Hierarchical clustering analysis of mAbs and viruses on the basis of their neutralization profiles showed a clear phenotypic separation between broad and off-track mAbs, with the latter neutralizing substantially fewer autologous viruses, but we could not attribute this to any genetic features of the mAbs. Both groups neutralized viruses with an SU-like C-strand, including the bNAb-initiating 34-week clones. All viruses neutralized by off-track antibodies were also sensitive to at least one broad mAb, suggesting that viral variants associated with the development of neutralization breadth also selected off-track mAbs. Indeed, clustering of broad and off-track mAbs within a single phylogenetic branch highlights the stochastic nature of mAb maturation toward breadth (**Fig. 4c**).

In conclusion, we identified 34-week viral variants, which we have termed bNAb-initiating Envs, that effectively engaged the UCA of the CAP256-VRC26 V1V2 lineage. Although low-frequency viral escape mutations at 27–30 weeks may suggest that CAP256-VRC26 antibodies were present earlier, the 34-week Envs nonetheless represent optimal priming immunogens for this lineage. Identification of rare bNAb-initiating Envs is likely to be of particular importance for V1V2 bNAb precursors, which are derived from a pool of rare B cells with long CDRH3 regions[8,18,22–26]. Second, we have defined a new mechanism for how accumulating viral variants contribute to bNAb development. Thus, viral escape creates multiple immunotypes, and in parallel SHM generates antibodies with differential abilities to engage these epitope variants. Those antibody sublineages that are able to tolerate variability at key epitope contacts will develop breadth (**Fig. 4d**). We note,

however, that viral diversity may also limit the evolution of less-tolerant mAbs (dead-end sublineages), or it may divert maturation of mAbs toward strain specificity (off-track mAbs) (**Fig. 4d**). This process, which provides a framework for vaccine design (**Supplementary Fig. 7**), is distinct from the multi-lineage cooperative pathway described for a CD4–binding site bNAb lineage[10], highlighting the complex and varied pathways to breadth. Future immunization strategies should therefore aim to include bNAb-initiating Envs to prime bNAb precursor B cells, as well as rationally verified Env variants as sequential boosts to mature the response to neutralization breadth.

METHODS

Methods and any associated references are available in the online version of the paper.

Accession codes. Antibody 454 sequencing reads have been deposited in the National Center for Biotechnology Information (NCBI) Sequence Read Archive (SRA) under the accession numbers SRR2126754 and SRR2126755. Viral V1V2 Illumina MiSeq sequencing reads have been deposited in the NCBI SRA under the BioProject accession number PRJNA294363. CAP256 34-week viral envelope sequences have been have been deposited with GenBank under the accession numbers KT698223–KT698227.

Note: Any Supplementary Information and Source Data files are available in the online version of the paper.

ACKNOWLEDGMENTS

We thank the participants in the CAPRISA 002 cohort for their commitment to attending the CAPRISA clinics in South Africa. Thanks to the CAPRISA 002 study team (including N. Naicker, V. Asari, N. Majola, T. Cekwane, N. Samsunder, Z. Mchunu, D. Nkosi, H. Shozi, S. Ndlovu, P. Radebe, K. Leask and M. Upfold) for managing the cohort and providing specimens. We are grateful to C. K. Wibmer for useful discussions. We thank P. Labuschagne, D. Matten and T. York for assistance with viral next-generation sequence analysis, R. Bailer and M. Louder for the CAP256-VRC26 UCA neutralization data against the large virus panel and J. Mulllikin and the US National Institutes of Health (NIH) Intramural Sequencing Center (NISC) Comparative Sequencing Program for antibody NGS data at 34 weeks. We are grateful to J. Baalwa, D. Ellenberger, F. Gao, B. Hahn, K. Hong, J. Kim, F. McCutchan, D. Montefiori, J. Overbaugh, E. Sanders-Buell, G. Shaw, R. Swanstrom, M. Thomson, S. Tovanabutra and L. Zhang for contributing the HIV-1 envelope plasmids used in our neutralization panel. The JC53bl-13 (TZM-bl) and 293T cell lines were obtained through the NIH AIDS Reagent Program, Division of AIDS, NIAID, NIH from J.C. Kappes, X. Wu and Tranzyme, Inc., and A. Rice, respectively. We acknowledge research funding from the Centre for the AIDS Programme of Research (CAPRISA) (S.S.A.K.), the South African Medical Research Council (MRC) SHIP program (P.L.M.), the NIH through a U01 grant (AI116086-01) (P.L.M.), the intramural research programs of the Vaccine Research Center and the National Institute of Allergy and Infectious Diseases (NIAID) (J.R.M.). CAPRISA is funded by the South African HIV/AIDS Research and Innovation Platform of the South African Department of Science and Technology, and was initially supported by the US NIAID, NIH, US Department of Health and Human Services grant U19 AI51794 (S.S.A.K.). Funding was received by J.N.B. and C.A. from the Columbia University-Southern African Fogarty AIDS International Training and Research Program through the Fogarty International Center, NIH grant 5 D43 TW000231 (to Quarraisha Abdool Karim). Additional fellowships included a University of the Witwatersrand Postgraduate Merit Award (J.N.B.), a Poliomyelitis Research Foundation PhD Bursary (J.N.B.), a National Research Foundation of South Africa Innovation PhD Bursary (J.N.B.), a National Research Foundation of South Africa Postdoctoral Fellowship (C.A.), and a Wellcome Trust Intermediate Fellowship in Public Health and Tropical Medicine, grant 089933/Z/09/Z (P.L.M.).

AUTHOR CONTRIBUTIONS

J.N.B., L.M. and P.L.M. designed the study, analyzed data and wrote the manuscript. C.A. and C.W. designed and performed viral NGS and analysis and edited the manuscript. N.A.D.-R. led the isolation of CAP256 mAbs. J.N.B. and O.K. performed neutralization experiments. C.A.S. and L.S. generated and analyzed antibody NGS data. J.N.B. and T.K. expressed and purified monoclonal antibodies. J.N.B. and D.K. generated single-genome sequences and viral envelope clones. G.B. developed computational tools to analyze NGS data, and assisted in the NGS analysis. J.G. assessed CAP256-VRC26 UCA neutralization of heterologous viruses. N.J.G. and the CAPRISA Study Team managed the CAPRISA cohort and contributed samples and data for CAP256. S.S.A.K., C.W. and L.M. established and led the CAPRISA cohort. C.W., N.A.D.-R., L.S., P.D.K., and J.R.M. contributed to data analysis and edited the manuscript.

COMPETING FINANCIAL INTERESTS

The authors declare no competing financial interests.

1. Gray, E.S. *et al.* HIV-1 neutralization breadth develops incrementally over 4 years and is associated with CD4+ T cell decline and high viral load during acute infection. *J. Virol.* **85**, 4828–4840 (2011).
2. Hraber, P. *et al.* Prevalence of broadly neutralizing antibody responses during chronic HIV-1 infection. *AIDS* **28**, 163–169 (2014).
3. Piantadosi, A. *et al.* Breadth of neutralizing antibody response to human immunodeficiency virus type 1 is affected by factors early in infection but does not influence disease progression. *J. Virol.* **83**, 10269–10274 (2009).
4. Sather, D.N. *et al.* Factors associated with the development of cross-reactive neutralizing antibodies during human immunodeficiency virus type 1 infection. *J. Virol.* **83**, 757–769 (2009).
5. Euler, Z. *et al.* Longitudinal analysis of early HIV-1-specific neutralizing activity in an elite neutralizer and in five patients who developed cross-reactive neutralizing activity. *J. Virol.* **86**, 2045–2055 (2012).
6. Walker, L.M. *et al.* A limited number of antibody specificities mediate broad and potent serum neutralization in selected HIV-1 infected individuals. *PLoS Pathog.* **6**, e1001028 (2010).
7. Doria-Rose, N.A. *et al.* Developmental pathway for potent V1V2-directed HIV-neutralizing antibodies. *Nature* **509**, 55–62 (2014).
8. Liao, H.X. *et al.* Co-evolution of a broadly neutralizing HIV-1 antibody and founder virus. *Nature* **496**, 469–476 (2013).
9. Mascola, J.R. & Haynes, B.F. HIV-1 neutralizing antibodies: understanding nature's pathways. *Immunol. Rev.* **254**, 225–244 (2013).
10. Gao, F. *et al.* Cooperation of B cell lineages in induction of HIV-1-broadly neutralizing antibodies. *Cell* **158**, 481–491 (2014).
11. Wibmer, C.K. *et al.* Viral escape from HIV-1 neutralizing antibodies drives increased plasma neutralization breadth through sequential recognition of multiple epitopes and immunotypes. *PLoS Pathog.* **9**, e1003738 (2013).
12. Moore, P.L. *et al.* Evolution of an HIV glycan-dependent broadly neutralizing antibody epitope through immune escape. *Nat. Med.* **18**, 1688–1692 (2012).
13. Moore, P.L. *et al.* Multiple pathways of escape from HIV broadly cross-neutralizing V2-dependent antibodies. *J. Virol.* **87**, 4882–4894 (2013).
14. Doria-Rose, N.A. *et al.* A new member of the V1V2-directed CAP256-VRC26 lineage that shows increased breadth and exceptional potency. *J. Virol.* (in the press).
15. Klein, F. *et al.* Antibodies in HIV-1 vaccine development and therapy. *Science* **341**, 1199–1204 (2013).
16. Kwong, P.D., Mascola, J.R. & Nabel, G.J. Broadly neutralizing antibodies and the search for an HIV-1 vaccine: the end of the beginning. *Nat. Rev. Immunol.* **13**, 693–701 (2013).
17. Sok, D. *et al.* Recombinant HIV envelope trimer selects for quaternary-dependent antibodies targeting the trimer apex. *Proc. Natl. Acad. Sci. USA* **111**, 17624–17629 (2014).
18. Walker, L.M. *et al.* Broad neutralization coverage of HIV by multiple highly potent antibodies. *Nature* **477**, 466–470 (2011).
19. Scheid, J.F. *et al.* Broad diversity of neutralizing antibodies isolated from memory B cells in HIV-infected individuals. *Nature* **458**, 636–640 (2009).
20. Mouquet, H. *et al.* Memory B cell antibodies to HIV-1 gp140 cloned from individuals infected with clade A and B viruses. *PLoS ONE* **6**, e24078 (2011).
21. Pappas, L. *et al.* Rapid development of broadly influenza neutralizing antibodies through redundant mutations. *Nature* **516**, 418–422 (2014).
22. Walker, L.M. *et al.* Broad and potent neutralizing antibodies from an African donor reveal a new HIV-1 vaccine target. *Science* **326**, 285–289 (2009).
23. Briney, B.S., Willis, J.R. & Crowe, J.E. Jr. Human peripheral blood antibodies with long HCDR3s are established primarily at original recombination using a limited subset of germline genes. *PLoS ONE* **7**, e36750 (2012).
24. Wardemann, H. *et al.* Predominant autoantibody production by early human B cell precursors. *Science* **301**, 1374–1377 (2003).
25. Jardine, J. *et al.* Rational HIV immunogen design to target specific germline B cell receptors. *Science* **340**, 711–716 (2013).
26. McGuire, A.T. *et al.* Engineering HIV envelope protein to activate germline B cell receptors of broadly neutralizing anti-CD4 binding site antibodies. *J. Exp. Med.* **210**, 655–663 (2013).

ONLINE METHODS

Study participant. CAP256 was part of the CAPRISA 002 Acute Infection study, a cohort of 245 high-risk, HIV-negative women that was established in 2004 in Durban, South Africa, for follow-up and subsequent identification of HIV seroconversion[27]. This HIV-infected individual was among the seven women in this cohort who developed neutralization breadth[1]. The CAPRISA 002 Acute Infection study was reviewed and approved by the research ethics committees of the University of KwaZulu-Natal (E013/04), the University of Cape Town (025/2004) and the University of the Witwatersrand (MM040202). CAP256 provided written informed consent. Randomization and blinding were not performed in this study.

V1V2 next-generation sequence library preparation. RNA extraction, cDNA synthesis and subsequent amplification were carried out as described previously[28], with the following modifications: A minimum of 5,000 HIV-1 RNA copies were isolated from longitudinal plasma, spanning 4 years of infection, using the QIAamp Viral RNA kit (Qiagen, Germany). The cDNA synthesis primer was designed to bind to the C3 region of the envelope (HXB2 gp160 position 1,094–1,118) and included a randomly assigned 9-mer tag (Primer ID method) to uniquely label each cDNA molecule, followed by a universal primer binding site to allow out-nested PCR amplification of cDNA templates (primers listed in **Supplementary Table 1**). First-round amplification primers were designed to amplify the V1 to V3 region of the envelope (HXB2 gp160 positions 332–358) and contained a template-specific binding region, followed by a variable-length spacer of 0–3 randomly assigned bases to increase sample complexity. In addition, PCR primers contained 5′ overhangs, introducing binding sites for the Nextera XT indexing primers (Illumina, CA) (**Supplementary Table 1**). The nested PCRs were carried out using the Nextera XT indexing kit. After indexing, samples were purified using the MinElute PCR Purification Kit (Qiagen, Germany), quantified using the Quant-iT PicoGreen dsDNA assay (Life Technologies, NY) and pooled in equimolar concentrations. The pooled amplicons were gel extracted using the QIAquick gel purification kit (Qiagen, Germany) to ensure primer removal and the final library submitted for sequencing on an Illumina MiSeq (San Diego, CA), using 2 × 300 paired-end chemistry.

V1V2 next-generation sequence analysis. Raw reads were processed using a local instance of Galaxy[29–31], housed within the University of Cape Town High-Performance Computing core. Read quality was assessed using fastqc (http://www.bioinformatics.babraham.ac.uk/projects/fastqc). Short reads (<150 bp) and low-quality data were filtered out using the Filter FASTQ (version 1.0.0) tool[32] with a minimum quality of Q35 for 3′ base trimming. Forward and reverse reads were joined using FASTQ joiner (version 2.0.0)[32]. A custom python script was used to bin all reads containing an identical Primer ID tag, to align the reads within each bin using MAFFT[33] and to produce a consensus sequence based on a majority rule. Sequences with just one Primer ID representative, as well as consensus sequences derived from less than three reads and those containing degenerate bases, were excluded and the remaining sequences from each time point were aligned with MAFFT, Muscle[34] or RAMICS[35]. The calculation of amino acid frequencies and Hamming distances (for each sequence relative to the consensus sequence from the first time point–inferred PI virus), were performed using custom python scripts. Amino acid frequency distributions were plotted using Prism 6 (GraphPad), whereas Hamming distances were plotted using the python library Matplotlib[36]. All custom scripts used in these analyses, including the Primer ID binning script, are available upon request from Gordon Botha (gbot300@gmail.com).

Single-genome amplification and sequencing. HIV-1 RNA was isolated from plasma using the Qiagen QIAamp Viral RNA kit and reverse transcribed to cDNA using SuperScript III Reverse Transcriptase (Invitrogen, CA). The envelope genes were amplified from single-genome templates[37], and amplicons were directly sequenced using the ABI PRISM BigDye Terminator Cycle Sequencing Ready Reaction kit (Applied Biosystems, Foster City, CA) and resolved on an ABI 3100 automated genetic analyzer. The full-length *env* sequences were assembled and edited using Sequencher version 4.5 software (Genecodes, Ann Arbor, MI). Multiple sequence alignments were performed using Clustal X (version 1.83) and edited with BioEdit (version 7.0.9.0) Sequence alignments were visualized using Highlighter for Amino Acid Sequences version 1.1.0 (beta). Selected amplicons were cloned into the expression vector pcDNA 3.1 (directional) (Life Technologies) by reamplification of SGA first-round products using Fusion enzyme (Stratagene) with the EnvM primer[38] and the directional primer EnvAStop[39]. Cloned *env* genes were sequenced to confirm that they exactly matched the sequenced amplicon, and assayed for function by transfection in 293T cells, as described below.

Site-directed mutagenesis. CAP256 15-wk SU was mutated at positions 169 and 166 by site-directed mutagenesis using the Stratagene QuikChange II kit (Stratagene) as described by the manufacturer. Mutations were confirmed by sequencing.

Antibody next-generation sequence analysis. NGS reads from each time point were processed with an antibodyomics approach described previously[7]. Reads with successfully assigned V and J genes, an in-frame junction and no stop codons were clustered at 97.25% nucleotide sequence identity with CD-HIT to account for possible sequencing error and singletons were discarded. For those remaining reads assigned to VH3-30, divergence from VH and identity to the previously determined UCA[7] were calculated with Clustalw2. Density plots for these sequences were generated using the kde2d function in R. A maximum likelihood tree was built using FastML as described[7]. The tree was collapsed for display by clustering CDRH3 sequences as described[7] using a 90% identity threshold and a minimum of three sequences to define a major branch.

Antibody expression. Equal quantities of antibody heavy and light chain plasmids were co-transfected into FreeStyle 293F cells (Life Technologies) using the PEIMAX transfection reagent (Polysciences). Monoclonal antibodies were purified from cell-free supernatants after 6 d using protein A affinity chromatography.

Neutralization assays. The JC53bl-13 (TZM-bl) and 293T cell lines, confirmed to be free of *Mycoplasma*, were cultured in DMEM (Gibco BRL Life Technologies) containing 10% heat-inactivated FBS and 50 μg/ml gentamicin (Sigma). Cell monolayers were disrupted at confluency by treatment with 0.25% trypsin in 1 mM EDTA (Gibco BRL Life Technologies). Env-pseudotyped viruses were obtained by co-transfecting the Env plasmid with pSG3ΔEnv[40], using the FuGENE transfection reagent (Roche) as previously described[1]. Neutralization was measured as described by a reduction in luciferase gene expression after single-round infection of JC53bl-13 cells with Env-pseudotyped viruses[1]. Titers were calculated as the reciprocal plasma dilution (ID_{50}) causing 50% reduction of relative light units (RLU). Viral and antibody hierarchical clustering based on neutralization profiles was performed using the Heatmap Hierachical Clustering tool on the LANL HIV sequence database http://www.hiv.lanl.gov/content/sequence/HEATMAP/heatmap.html.

Images. Electron microscopy and protein structure representations were created with Chimera 1.5.3rc and The PyMOL Molecular Graphics System, Version 1.3r1edu, Schrödinger LLC. Neutralization images were created in GraphPad Prism6, sequence alignments were made with BioEdit[41] and phylogenetic trees were edited in FigTree 1.4.2.

27. van Loggerenberg, F. *et al.* Establishing a cohort at high risk of HIV infection in South Africa: challenges and experiences of the CAPRISA 002 acute infection study. *PLoS ONE* **3**, e1954 (2008).
28. Jabara, C.B., Jones, C.D., Roach, J., Anderson, J.A. & Swanstrom, R. Accurate sampling and deep sequencing of the HIV-1 protease gene using a Primer ID. *Proc. Natl. Acad. Sci. USA* **108**, 20166–20171 (2011).
29. Goecks, J., Nekrutenko, A., Taylor, J. & Galaxy, T. Galaxy: a comprehensive approach for supporting accessible, reproducible, and transparent computational research in the life sciences. *Genome Biol.* **11**, R86 (2010).
30. Blankenberg, D. *et al.* Galaxy: a web-based genome analysis tool for experimentalists. *Curr. Protoc. Mol. Biol.* **89**, 19.10.1–19.10.21 (2010).

doi:10.1038/nm.3963

31. Giardine, B. *et al.* Galaxy: a platform for interactive large-scale genome analysis. *Genome Res.* **15**, 1451–1455 (2005).
32. Blankenberg, D. *et al.* Manipulation of FASTQ data with Galaxy. *Bioinformatics* **26**, 1783–1785 (2010).
33. Katoh, K. & Standley, D.M. MAFFT multiple sequence alignment software version 7: improvements in performance and usability. *Mol. Biol. Evol.* **30**, 772–780 (2013).
34. Edgar, R.C. MUSCLE: multiple sequence alignment with high accuracy and high throughput. *Nucleic Acids Res.* **32**, 1792–1797 (2004).
35. Wright, I.A. & Travers, S.A. RAMICS: trainable, high-speed and biologically relevant alignment of high-throughput sequencing reads to coding DNA. *Nucleic Acids Res.* **42**, e106 (2014).
36. Hunter, J.D. Matplotlib: A 2D graphics environment. *Comput. Sci. Eng.* **9**, 90–95 (2007).
37. Salazar-Gonzalez, J.F. *et al.* Deciphering human immunodeficiency virus type 1 transmission and early envelope diversification by single-genome amplification and sequencing. *J. Virol.* **82**, 3952–3970 (2008).
38. Gao, F. *et al.* Molecular cloning and analysis of functional envelope genes from human immunodeficiency virus type 1 sequence subtypes A through G. The WHO and NIAID Networks for HIV Isolation and Characterization. *J. Virol.* **70**, 1651–1667 (1996).
39. Kraus, M.H. *et al.* A rev1-vpu polymorphism unique to HIV-1 subtype A and C strains impairs envelope glycoprotein expression from rev-vpu-env cassettes and reduces virion infectivity in pseudotyping assays. *Virology* **397**, 346–357 (2010).
40. Wei, X. *et al.* Antibody neutralization and escape by HIV-1. *Nature* **422**, 307–312 (2003).
41. Hall, T.A. BioEdit: a user-friendly biological sequence alignment editor and analysis program for Windows 95/98/NT. *Nucl. Acids. Symp. Ser.* **41**, 95–98 (1999).